

Supporting Information

Kang et al. 10.1073/pnas.0915085107

SI Text

Materials and Methods. Organ harvesting and preparation of cell-free extracts. *Cry1*^{-/-}*Cry2*^{-/-} mice in C57BL/6J background were generated previously in our lab (1, 2), and wild-type animals (8–10 weeks old C57BL/6J male mice) were purchased from the Jackson Laboratory (Bar Harbor, ME). Mice were maintained on a light/dark 12:12 schedule for at least for 2 weeks before sacrifice. ZT0 is the time of light-on (0700) and ZT12 is the time of light-off (1900). Genomic DNA prepared from the tail was analyzed for genotyping using polymerase chain reaction with appropriate primers as previously described (3) (Fig. S7). The mice were handled in accordance with the guidelines of NIH and the University of North Carolina School of Medicine. At the indicated times, the mice were sacrificed by carbon dioxide exposure, tissues were removed and washed extensively with cold phosphate buffered saline (PBS), and then frozen in liquid nitrogen. Frozen tissue was pulverized using a porcelain mortar and pestle under liquid nitrogen, and cell-free extract (CFE) was prepared as described previously (4). Due to significant contamination of the liver CFE with nonspecific DNase activity, the liver was further treated by chopping into less than 2 mm size pieces and incubating in a red blood cell lysis buffer (Sigma) to generate excision repair proficient extracts. Note that because of the different preparation procedures for testis and liver extracts, only the absolute values of the repair activities from the same organ harvested at different times of the day can be compared. Hence, even though testis extracts exhibited overall higher activities than liver extracts at all time points, testis is not necessarily more active in excision repair than the liver.

Preparation of DNA substrates containing a GpTpG cisplatin intrastand adduct at a unique site for excision assay. Previously described procedures (5) were used for preparation of 140-bp linear duplexes or 2.9 kb plasmid DNA. Oligomers were obtained from The Midland Certified Reagent Company and Integrated DNA Technologies. Oligomers were treated with cisplatin (Sigma) at a 10:1 molar ratio of aquated platinum to DNA as described (6). Analysis of the treated oligomers indicated that 85–90% of the molecules were platinated. Damaged oligomers were 5' radiolabelled with [γ -³²P ATP] (7000 Ci/mmol, MP Biomedicals) and used for substrate preparation. The linear duplex substrate was prepared by annealing and ligation of the platinated oligomer, 5'-TCT GTG CAC TCT (adducted nucleotides underlined), with five other complementary and partially overlapping oligomers. Because of the significant exonuclease contamination in the liver CFE, which degraded the linear substrate, we generated a circular substrate by second strand DNA synthesis of pIBI25 single-stranded template DNA using a platinated 26-mer, 5'-GCT GTT TCC TGT GTG AAA TTG TTA TC, as primer. Because of its availability in high quantities, this substrate was used with some of the repair assays with the testis extracts as well.

DNA excision repair assay. Nucleotide excision repair activity with the tissue extracts was carried out with CFE as reported previously (4). A schematic of the excision repair assay is shown in Fig. S1. Either 10 fmol of duplex (140-bp) or circular plasmid DNA (2.9 kb) with a platinum (GpTpG) diadduct in the center and ³²P-label at the 4th or 13th phosphodiester bond 5' to the damage was incubated with 100 μ g of CFE in 25 μ l excision buffer at 30°C for 1 h. Only the regions of the excision repair gels containing the product (24–32 nt range) are shown in the manuscript, and the entire gels are shown in Fig. S2. Quantification of exci-

sion products was performed using ImageQuant 5.2 software (Molecular Dynamics).

Immunoblotting. Conventional immunoblotting procedures were used to determine the levels of a select number of proteins involved in the circadian clock, nucleotide excision repair, and DNA damage checkpoint. The following antibodies were obtained from commercial sources: XPB, XPC, XPD, ATR, RPA70, CHK1, CHK2, RAD1, RAD9, Actin, PCNA, Cyclophilin-B (Santa Cruz Biotechnology), XPA (Kamiya biomedical), XPE (Invitrogen), XPF (Abcam), HERC1, HERC2 and XPG (Bethyl Laboratory), ATM (Novus Biologicals), DNA-PKcs (Neomarkers), ATRIP (Zymed), TOPBP1, ORC2 and H2A.X (Millipore), GAPDH (Cell Signaling Technology), RPA32 (Calbiochem), Clock (Affinity BioReagents), Platinum GpG (OncoLyze), and MDM2 and Flag M2 (Sigma). The *Cry1* and *Cry2* antibodies were generated in our laboratory (7, 8). We note that XPA, even under denaturing conditions of SDS-PAGE, assumes two alternative conformations, and as a consequence it appears as a “doublet” in some of the SDS-PAGE gels (9).

RT-PCR. Total RNA from mouse liver and testis, isolated using RNeasy Plus Mini (Qiagen), was subjected to reverse transcription using ImProm-II Reverse Transcription System (Promega). *Xpa* (NM_011728.2, expected size of PCR product is 556 bp) and β -*Actin* (NM_007393.3, expected size of product is 359 bp) were amplified in the same tube and resolved in a 1.2% agarose gel stained with SYBR-gold and visualized under a UV transilluminator. The following primers were used for PCR (for *Xpa* 5':CAAAGGTGGCTTCATTTTAG and 3':GGTACATGCATCTTCTAAG; and for β -*Actin* 5':GTTCCGATGCCCTGAGGCTC and 3':CACTTGCGGTGCACGATGGA).

Cell culture and siRNA transfection. HEK293T (ATCC, American Type Culture Collection), A549, and Rat1 cell lines (obtained from the University of North Carolina Lineberger Comprehensive Cancer Research Center Tissue Culture Facility) were grown in Dulbecco's Modified Eagle Medium (DMEM, Gibco) supplemented with 10% fetal bovine serum and 100 U/ml penicillin G and 0.1 mg/ml streptomycin. For the analysis of protein stability, cells were treated with 20 μ g/ml cycloheximide (Sigma) or 40 μ M MG132 (Sigma) for the indicated times. For immunofluorescence staining, cells were grown on a glass chip coated with poly-D-lysine and laminin (BD Biosciences). DharmaFECT reagent (Dharmacon) was used according to the manufacturer's directions for transfection of ON-TARGET plus SMARTpool siRNA duplexes obtained from Dharmacon [*HERC1* (L-007181-00-0005), *HERC2* (L-007180-00-0020), or *Cyclophilin-B* (D-001820-01-20) as a control].

Proteomics. Tetracycline-inducible Flag-XPA HEK293/FRT cells were generated according to the manufacturer's instructions (Invitrogen). Full-length human *XPA* cDNA was amplified from pRSET-His⁶-XPA (10) by PCR with oligos 5'-CTAGGAG-GATCCACCATGGATTACAAAGACGATGACGA-CAAGGCGGGCGGCCGACGGGGCTTTG-3' and 5'-CGCGCTCGAGTCACATTTTTTTCATATGTCAG-3' for subcloning into the BamHI and XhoI sites of pcDNA5/FRT Flp-In™ expression vector (Invitrogen). Flag-XPA was immunoprecipitated with anti-Flag agarose (Sigma) as previously described (11). Briefly, $\sim 2 \times 10^8$ cells were induced with 1 μ g/ml

of tetracycline for 24 h, lysed with TBS buffer (50 mM Tris-HCl pH 7.5, 150 mM NaCl) containing 0.5% NP-40, and purified with 80 μ l of Flag-agarose. After extensive washing with TBS buffer, the bound proteins were eluted with TBS buffer containing 0.3 mg/ml Flag-peptide (Sigma), resolved on a 4–12% NuPAGE Bis-Tris Gel, and visualized by SYPRO Ruby staining (Invitrogen). Mass spectrometric analysis was performed by the University of North Carolina Mass Spectrometry Core Facility.

Extraction of subcellular fractions. Cytoplasmic and nucleoplasmic extracts were isolated as described previously (12). A chromatin-enriched fraction was prepared using the pellet obtained following the extraction of the nucleoplasm by treatment with 10 U of DNase I (Promega) and 100 U of micrococcal nuclease (USB) for 30 min at 30 °C. Each fraction was analyzed by SDS–PAGE followed by Ponceau S staining and immunoblotting.

Immunofluorescence staining. Immunofluorescence was performed as described previously (13). Cells grown on cover slips were fixed in 4% (w/v) paraformaldehyde (USB) in PBS for 20 minutes at room temperature. Cells were washed three times with PBS containing 0.1% Triton X-100 (PBST), permeabilized in 0.5% (v/v) NP-40 in PBS for 10 minutes, washed once in PBST, and blocked with 3% (w/v) bovine serum albumin in PBS for 30 minutes. Primary antibodies were incubated for 1 h at room temperature and washed three times with PBST. After incubation with the appropriate secondary antibody, the cover slip was washed three times and embedded in Vectashield (Vector Laboratories). Images were captured using a Nikon TE2000U fluorescence microscope.

Ubiquitination assay. HERC2 immunoprecipitated from A549 cells was used in the ubiquitination assay. Briefly, cells were lysed by incubation with lysis buffer containing 50 mM Tris pH 7.6, 150 mM NaCl, 0.5% NP-40, phosphatase inhibitor cocktail (Sigma), and protease inhibitor tablet (Roche) for 30 minutes at 4 °C. 2 mg of lysates and 2 μ g of the appropriate antibody, pre-conjugated with protein A agarose (Sigma), were incubated for 3 hours or overnight at 4 °C. Immunoglobulin G (Santa Cruz Biotechnology) was used as a negative control. 1.5 ng of E1 (UBE1), 10 ng of E2 (UbcH5a), 500 ng of HA-ubiquitin, and 500 ng of purified Flag-XPA were incubated in a buffer containing 50 mM Tris pH 7.6, 5 mM MgCl₂, 0.6 mM DTT, and 2 mM ATP for 30 min at 30 °C. Recombinant UBE1, GST-UbcH5a, and HA-ubiquitin were purchased from Boston Biochem.

DNA slot blot. A549 cells grown in 6-well plates were treated with the indicated concentrations of cisplatin for 3 hours followed by washing with fresh media and further incubation for the indicated times before harvesting. Genomic DNA was prepared using QIAamp DNA Mini kit (Qiagen), and 1 μ g of DNA was vacuum-transferred to nitrocellulose membrane using BioDot SF Microfiltration apparatus (BioRad). DNA was crosslinked to the membrane by incubation at 80 °C for 2 hours under vacuum. A monoclonal antibody which recognizes Pt-(GpG) adducts (14) (Oncolyze) was used to detect the remaining amounts of platinum in the genomic DNA. The DNA bound to the membrane was detected with SYBR-Gold dye and used as loading control.

- Vitaterna MH, Selby CP, Todo T, Niwa H, Thompson C, et al. (1999) Differential regulation of mammalian period genes and circadian rhythmicity by cryptochromes 1 and 2. *Proc Natl Acad Sci USA* 96: 12114–12119
- Selby CP, Thompson C, Schmitz TM, Van Gelder RN, Sancar A (2000) Functional redundancy of cryptochromes and classical photoreceptors for nonvisual ocular photoreception in mice. *Proc Natl Acad Sci USA* 97: 14697–14702
- Ozturk N, Lee JH, Gaddameedhi S, Sancar A (2009) Loss of cryptochrome reduces cancer risk in p53 mutant mice. *Proc Natl Acad Sci USA* 106: 2841–2846
- Kang TH, Reardon JT, Kemp M, Sancar A (2009) Circadian oscillation of nucleotide excision repair in mammalian brain. *Proc Natl Acad Sci USA* 106: 2864–2867
- Reardon JT, Sancar A (2006) Purification and characterization of *Escherichia coli* and human nucleotide excision repair enzyme systems. *Methods Enzymol* 408: 189–213
- Vaisman A, Lim SE, Patrick SM, Copeland WC, Hinkle DC, et al. (1999) Effect of DNA polymerases and high mobility group protein 1 on the carrier ligand specificity for translesion synthesis past platinum–DNA adducts. *Biochemistry* 38: 11026–11039
- Partch CL, Shields KF, Thompson CL, Selby CP, Sancar A (2006) Posttranslational regulation of the mammalian circadian clock by cryptochrome and protein phosphatase 5. *Proc Natl Acad Sci USA* 103: 10467–10472
- Gauger MA, Sancar A (2005) Cryptochrome, circadian cycle, cell cycle checkpoints, and cancer. *Cancer Res* 65: 6828–6834
- Miyamoto I, Miura N, Niwa H, Miyazaki J, Tanaka K (1992) Mutational analysis of the structure and function of the xeroderma pigmentosum group A complementing protein. Identification of essential domains for nuclear localization and DNA excision repair. *J Biol Chem* 267: 12182–12187
- Mu D, Hsu DS, Sancar A (1996) Reaction mechanism of human DNA repair excision nuclease. *J Biol Chem* 271: 8285–8294
- Lindsey-Boltz LA, Wauson EM, Graves LM, Sancar A (2004) The human Rad9 checkpoint protein stimulates the carbamoyl phosphate synthetase activity of the multifunctional protein CAD. *Nucleic Acids Res* 32: 4524–4530
- Kang TH, Park DY, Choi YH, Kim KJ, Yoon HS, et al. (2007) Mitotic histone H3 phosphorylation by vaccinia-related kinase 1 in mammalian cells. *Mol Cell Biol* 27: 8533–8546
- Kang TH, Park DY, Kim W, Kim KT (2008) VRK1 phosphorylates CREB and mediates CCND1 expression. *J Cell Sci* 121: 3035–3041
- Liedert B, Pluim D, Schellens J, Thomale J (2006) Adduct-specific monoclonal antibodies for the measurement of cisplatin-induced DNA lesions in individual cell nuclei. *Nucleic Acids Res* 34: e47

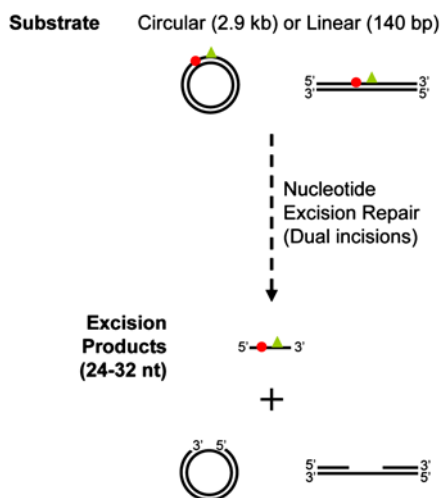


Fig. S1. Schematic diagram to measure excision repair activity (dual incisions) with cell-free extract (CFE) from mouse tissues. Radiolabelled (red dot) and (green triangle) substrate as a form of either circular plasmid DNA (2.9 kb, pBI25) or linear duplex DNA (140 bp) was incubated with CFE and the excision repair activity was measured by detecting 24–32 nucleotide-long excision products.

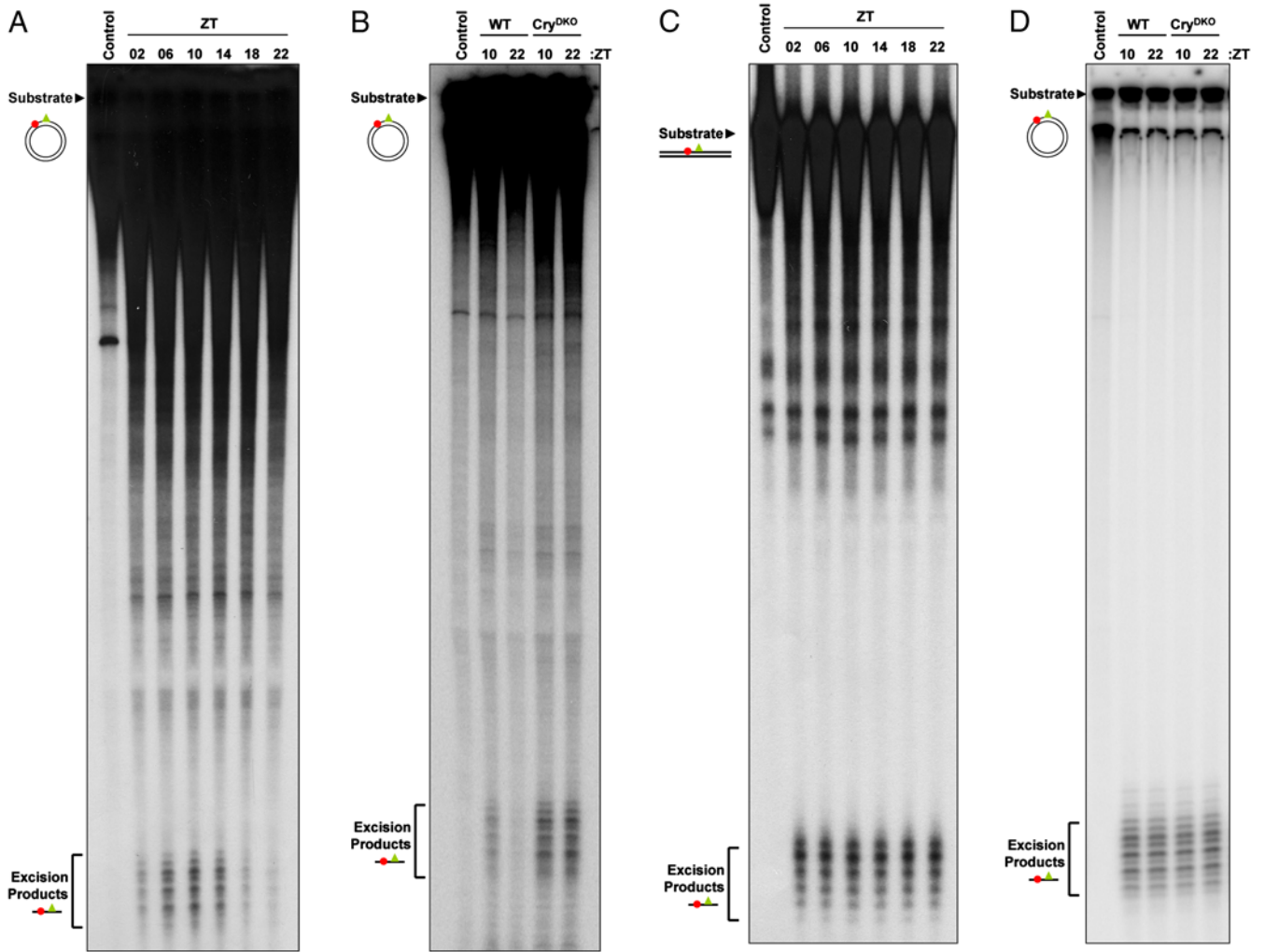


Fig. S2. Full images of excision repair gels. (A) Gel from Fig. 1A, (B) Gel from Fig. 1E, (C) Gel from Fig. 2A, and (D) Gel from Fig. 2D.

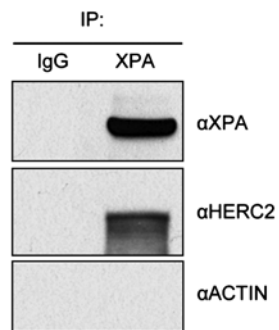


Fig. S3. Interaction of XPA and HERC2 in A549 cells. HERC2 association with XPA was confirmed by XPA immunoprecipitation (IP) followed by immunoblotting with HERC2 antibody. ACTIN was used as a nonbinding protein with XPA, and IP with mouse IgG1 was included as a negative control for the IP.

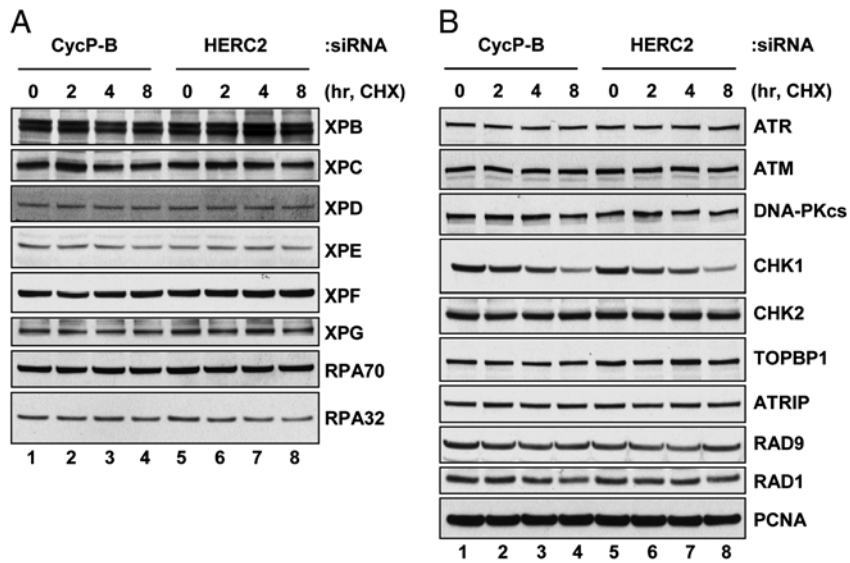
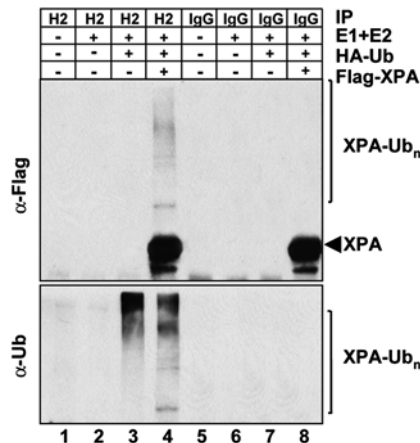


Fig. S4. Cells in which HERC2 or cyclophilin-B (CycP-B) were downregulated by siRNA were incubated with cycloheximide (CHX) for the indicated times and the levels of the proteins were probed by immunoblots. (A) The other core repair factors and the excision repair accessory protein XPE (DDB2) were not affected by HERC2 downregulation. (B) With the exception of CHK1, all checkpoint proteins tested are quite stable, maintaining essentially the same level for 8 h after the start of CHX treatment. Importantly, even though we find that CHK1 is unstable, its degradation is not affected by the presence or absence of HERC2.



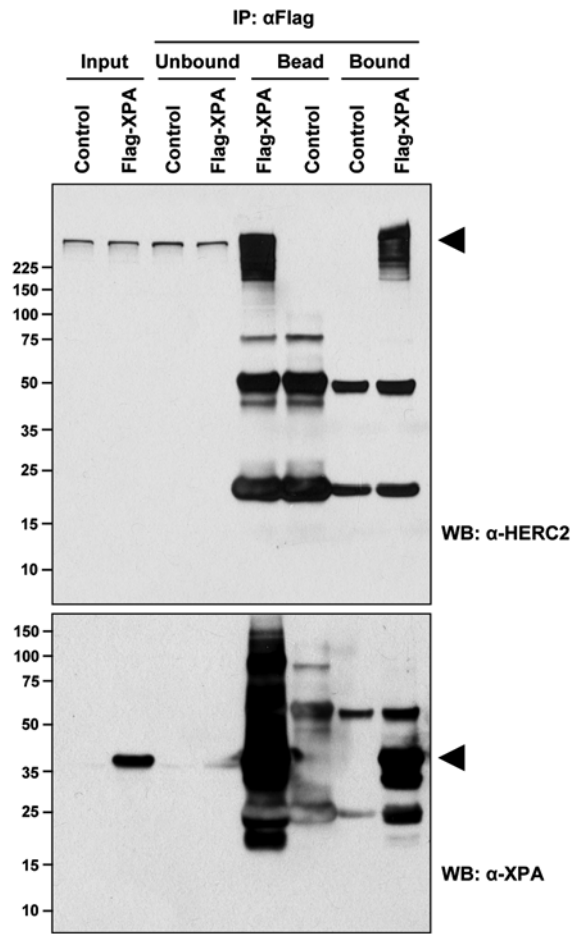


Fig. S6. Full gel images of immunoblotting of HERC2 and XPA used in the Fig. 4B to show the specificity of these antibodies.

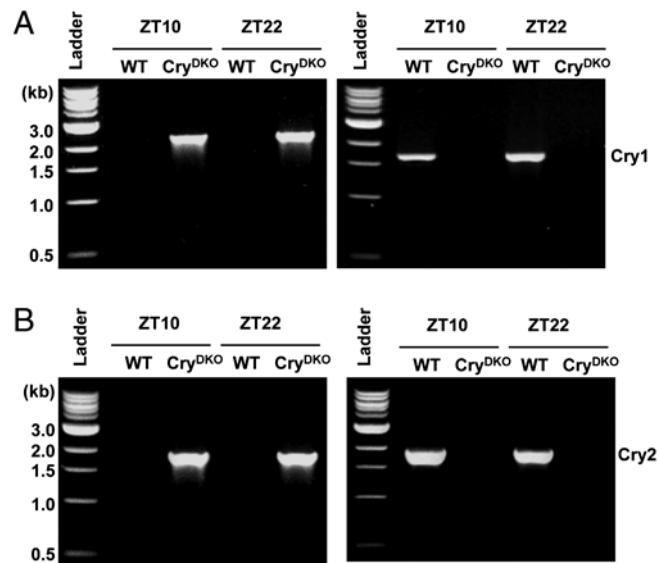


Fig. S7. Genotyping of mice used in this study. Genomic DNA from the tail of wild-type (WT) and $Cry1^{-/-}Cry2^{-/-}$ (Cry^{DKO}) were used for PCR amplification of both Cry1 (A) and Cry2 (B) with primers specific for WT (right panels) and Cry^{DKO} (left panels).

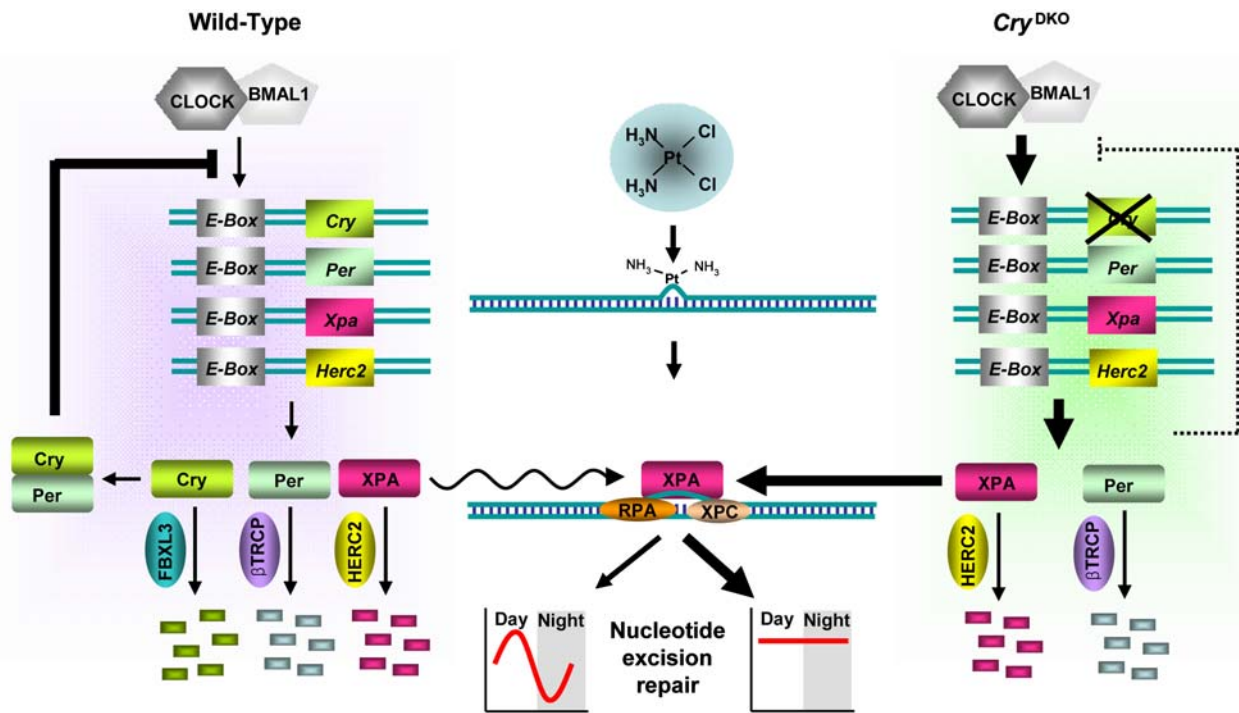


Fig. S8. Model for cryptochrome/circadian clock control of cisplatin-DNA adduct repair. In wild-type mice, the core clock proteins Clock-Bmal1 activate the transcription of *Per1/2* and *Cry1/2* genes. The *Per* and *Cry* proteins, after a time lag, enter the nucleus and inhibit Clock-Bmal1 activity and hence their own transcription (core circadian clock). In addition, Clock-Bmal1 activates the transcription of clock-controlled genes such as the nucleotide excision repair gene *Xpa*. The ubiquitination of *Crys* by Fbxl3 and *Pers* by β TRCP leads to degradation of these proteins and hence contributes to the oscillatory pattern of repression and generation of the circadian rhythm. Similarly, ubiquitination of XPA by HERC2 contributes to robust circadian oscillation of XPA levels (*Sinusoidal Arrow*) and hence of excision repair capacity. In cryptochromeless mice (*Cry^{DKO}*) there is only modest or no inhibition of Clock-Bmal1 complex by *Per*, and as a consequence Clock-Bmal1 controlled genes including *Xpa* are expressed at high levels at all times. Even though XPA is still ubiquitinated and degraded in *Cry^{DKO}* mice, the XPA level is higher than the wild-type leading to a constant and elevated level of XPA (*Straight Thick Arrow*) and of excision repair of bulky adducts such as those caused by cisplatin that is constant throughout the day.